Original scientific paper
UDC 631.181:635.655]:620.179.13

INVESTIGATION OF SOY MILK DEPOSITED ON STAINLESS STEEL BY INFRARED THERMOGRAPHY

Taweepol Suesut[1*], Maethinee Songthai[1], Navaphattra Nunak[1]

[1]Faculty of Engineering, King Mongkut's Institute of Technology Ladkrabang, Bangkok 10520, Thailand

[*]e-mail: taweepol.su@kmitl.ac.th

Abstract

This paper proposes a real-time investigation of soy milk deposited on stainless steel surface (SS) during the heating process by considering the relationship between emissivity and mass of soils on the surface using a thermal image processing technique. The understanding on organic fouling behavior is an important step leading to the optimum cleaning operations.

The mass of soy milk deposited on SS during heating process at the temperature of 75°C for 180 min was measured by the weighing method and compared to the emissivity values analyzed from the infrared thermography in real-time. Two different types of stainless steel grades (AISI 304 and 316) with various average surface roughness (R_a) values (0.4, 0.8 and 3.2 µm) were carried out.

Emissivity values of sample plates which soil deposited on the surface, were obtained from the real-time processing of a thermo-map of soil film compared to the temperature of a reference surface (known emissivity value). Applying this technique to all conditions, it was found that the increasing of emissivity values of sample plates as the amount of soil film on SS increased could be detected in real-time for both SS grades. The emissivity of SS having soil on the surface was higher than a clean SS since the soil film on the SS caused the roughness of surface changed. It could also detect that emissivity values of both SS grades had no significantly difference at the same R_a.

From the detection of soy milk deposited on SS using the real-time thermal image processing acquired from infrared camera during heating process, it could be concluded that the proposed technique was possible to investigate the accumulation of soy milk and other soil types on the surface.

Key words: *Infrared thermography, soy milk, fouling, average roughness, real-time thermal image processing*

1. Introduction

Stainless steel is the most widely used food contact material in the food industry, because it is a: non-toxic, durable, corrosion resistant material, resistant to disinfectants or cleaning agents and material with good cleaning properties. The American Iron and Steel Institute (AISI) classifies grades of stainless steel based on internal components such as: chromium, nickel, molybdenum, etc. The most widely used grades are austenitic stainless steel AISI 304 and AISI 316 [1]. According to the legislation on food contact surfaces (Directive 2006/42/EC) [2], besides the materials issues, the characteristics of surface, e.g. smoothness also need to be considered. Food contact surface can be a source of contamination from microorganisms and food spoilage to food product affecting to the safety of consumers. Other standards and organizations also concerned about the food safety regarding food equipment and food machinery are: ISO 14159, EN 1672-2, International Association of Food Industry Suppliers (IAFIS), and European Hygienic Engineering & Design Group (EHEDG). Most of them describe the smoothness of surface exposing to food area from the aspect of average roughness (R_a). EHEDG recommended that the food contact surface, whether in the dairy or other food industries, should have a surface finish of 0.8 µm R_a [3]. Many researchers have found that the surface roughness is an important factor that can affect the adhesion of bacteria, soil or other fluid agents on the surface [4, 5, 6, and 7]. Cross-contamination by pathogenic microorganisms often is caused by the organic substances, e.g. fat, protein, etc. that are deposited on the surface.

There are several methods to observe organic substances deposited on the stainless-steel surface such as: visual inspection, X-Ray Fluorescence (XRF), Ion Chromatography (IC), Optical Microscopy (OM), Inductively Coupled Plasma Optical Emission Fourier Transform Infrared Spectroscopy (FTIR), X-Ray Diffraction (XRD), and Atomic Absorption Spectroscopy (AAS) [8, and 9]. Visual inspection with the human eyes is an easy method, but it is difficult to make decisions because of the difference of experiences, while other techniques are complicated and requiring high operational and maintenance cost. Nowadays, some of the researchers have proposed the infrared thermography technique for the real-time detecting or monitoring of food products quality in many food industries [10, 11]. Since the infrared thermography is a rapid and non-contact temperature measurement technique, it can benefit to the food processing, especially from the food safety point of view, e.g. the controlling of hazards.

Some researchers have applied a surface radiative property of each object, called emissivity (ε), to differentiate the quality of products or types of products. This property depends on: material type, surface characteristic, angle and direction of emission, wavelength or spectral of infrared, and surface temperature [12, and 13]. In 2015, Ndukaife *et al.*, [10] applied an infrared thermography for characterization of fouling on flat sheet membrane surface. They found that the thickness of fouling was relevant to the emissivity value measured on the membrane surfaces. Several researchers have designed the equipment set with different heating techniques for emissivity measurement such as: Marinetti and Cearatto [14], Nunak *et al.*, [15], Suesut *et al.*, [16], Lopez *et al.*, [17], and Yu *et al.*, [18]; however, there are no any techniques applied for the real-time measurement. Although in the last years, the real-time image processing by computer vision with an optical camera has been used in the food industry for many applications, e.g. quality evaluation, identification, and grading of products [19], studies on a real-time infrared thermography processing of food processing are limited.

Therefore, this study was aimed to develop an experimental setup with the thermal image processing procedure for investigation the organic foulants deposited on the surface in real-time. The heating process of soy milk was used to be a case to study the organic fouling behavior on SS AISI 304 and 316 with different R_a values.

2. Materials and Methods

2.1 Creating the soy milk film

Soy milk with 25% solids content was prepared from soaked beans ground and heated with water at 95 ^{0}C in the soy milk making machine (PHILIPS model HD 2072) for 45 minutes. Then soy milk was poured into the chamber of experimental setup (Figure 1) which maintained the temperature at 75 ^{0}C. The test stainless-steel plates (wide: 4 cm, length 10 cm, AISI 304 with 0.4, 0.8, and 3.2 µm R_a and AISI 316 with 0.4 and 0.8 µm R_a) were pre-cleaned before soiling with water and ethanol. For organic fouling process the sample plate was placed on the test rig and the soy milk was flowed down over the SS for 180 min. The soiling behavior of soy milk was monitored in the test rig and where thermal image processing was performed immediately. Three replicates were carried out for each condition.

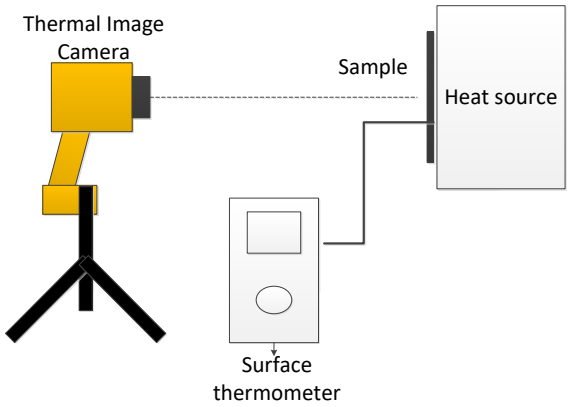

Figure 1. The conventional emissivity measurement using infrared camera

2.2 Emissivity measurement using infrared camera

The emissivity (ε) is a surface radiative property, which relates to the amount of radiation from the surface of an object. Generally, a different material has a different emissivity. The conventional emissivity measurement technique [14, 15, and 16], consists of: infrared camera, surface thermometer, sample, and heat source as shown in Figure 1. The environment such as room temperature and reflected sources must be controlled. This method is comprised of the following procedures: firstly, the sample is mounted to the heat source, which is set the temperature to be much more than the room temperature; then, the surface thermometer and thermal image camera are used to measure the sample surface temperature; finally, the ε value of the sample can be obtained by adjusting of ε value on the thermal image camera until the temperature measured from surface thermometer and thermal image camera was equal. This method is manual operation that cannot perform on-line measurement or collecting data in real-time.

2.3 The proposed emissivity measurement

Surface thermometer was not applied to the proposed method, but the reference material, known emissivity, was used instead. In this study black plastic tape (ε= 0.95) was used as a reference object. Its emissivity was

configured as the setting parameter in the infrared camera to measure the actual temperature of sample. Then emissivity value of sample surface (ε_s) can be calculated using equation (1)

$$\varepsilon_S = \frac{\varepsilon_{Ref} T_M^4}{T_S^4} \quad (1)$$

where: ε_{Ref} is the emissivity of reference material (black plastic tape), T_M is the temperature measured from the sample, T_S is the surface temperature measured from the reference material as shown in Figure 2. This technique is possible to apply the on-line measurement using real-time thermal image processing and benefits for continuing emissivity measurement.

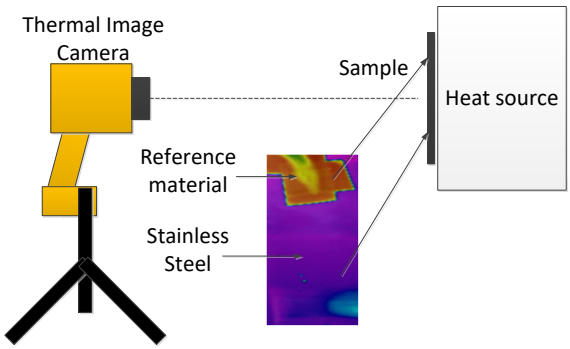

Figure 2. The proposed emissivity measurement using infrared camera

2.4 Experiment setup

The experimental setup (Figure 3) consisted of: an infrared camera, tripod, water bath, black plastic tape (referent surface), and the circulating pumps. When the soy milk was circulated over SS at the temperature of 75 ^{0}C, the deposition of organic fouling was created. Sample plate installed at the test rig must be a thin-flat plate as the reference material in order to obtain the homogenous temperature. The thermal image camera (Model FLIR A315, USA) having a temperature measurement range of -20 ^{0}C - 120 ^{0}C, the accuracy of ±2 ^{0}C, and the thermal sensitivity of 0.05 ^{0}C at 30 ^{0}C, was used in this study. The thermal image camera was calibrated with a blackbody (model 9132, HART Scientific, USA) before performing the experiments. The thermal detector is a focal plane array, 320 x 240 pixels with a 25^0(horizontal) x 18.8^0 (vertical) field of view, spatial resolution (IFOV) of 1.36 mRad at the minimum focus distance of 40 cm. The FLIR A315 thermal image camera provides the Gig E vision interface which can be performed real-time image processing by LabView 2014 with vision module software from National Instrument Corporations, USA.

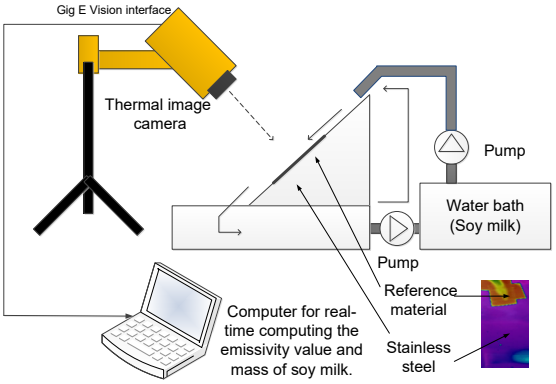

Figure 3. Experimental set up

A computer vision system for real-time computing was used to determine the quantity of soy milk deposited on SS by measuring the emissivity. The processing procedure started from acquiring thermal image from the object via Gigabit ethernet (Gig E) as shown in Figure 4. Then, thermal image processing was performed as the following steps:

Step 1: Thermal images were enhanced the quality of images by smoothing filter to reduce noise on images.

Step 2: Region of Interest (ROI) based processing was applied for segmentation of the thermal image into two parts: reference material area and sample area (SS with organic fouling from soy milk).

Step 3: Converting color pixels into temperature was implemented by matching color of each pixel with the temperature level.

Step 4: Averaged surface temperature was calculated from each pixel in each ROI.

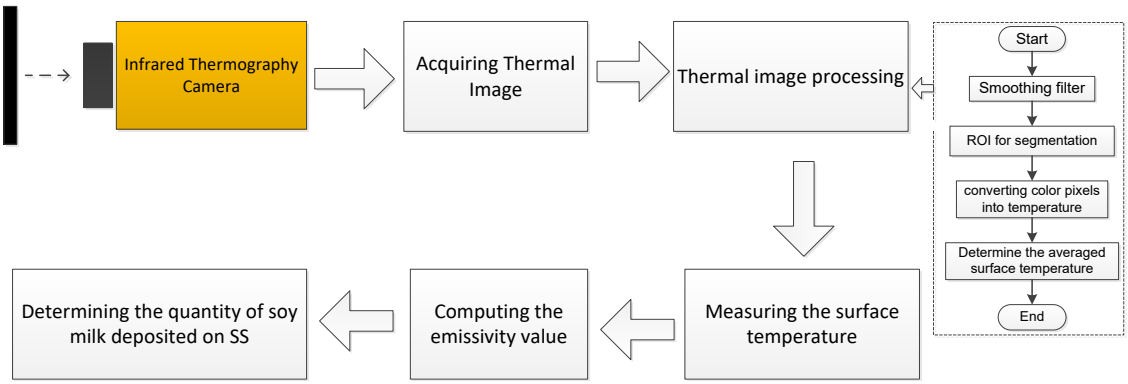

Figure 4. Processing procedure of infrared thermography

Afterwards, the ε value of sample plates at different locations of ROI on the thermal image was computed in real- time from surface temperatures using equation (1). Before determining the quantity of soy milk deposited on SS, the experimental data must be collected and analyzed to create the calibration curve. Finally, the soy milk deposited on the SS could be easily explained by monitoring the changes of ε values of the tested surface with time.

Figure 5 illustrated the example of infrared thermography having 9 ROIs on the image. ROI 1 presented the emission area of reference material and ROIs 2 - 9 presented the emission area of soiling. As the ε value of reference surface was set in the infrared camera, temperature (73.77 ^{0}C) displayed on the ROI 1 was the real value. Temperatures displayed on ROIs 2 - 9 were lower than the one on the ROI 1. This could be explained from the deposition of soy milk deposits on the surface. Since the emissivity of clean stainless steel (ε~0.3 - 0.6) was lower than the one of reference surface and soy milk film (ε~0.95), the emission of soiling surface was in between emission of clean SS and reference surface as shown the temperature at different ROIs in Figure 5 (a). However, describing soy milk deposited on SS using temperature or thermo-map was quite difficult to understand. Hence, it could be suggested to present with ε values as shown in Figure 5 (b).

2.5 Data analysis

Excel (Microsoft office 2010) was used for ANOVA statistics. The results were determined from triplicate measurements. Data analyzed by analysis of variance and means was separated by Tukey's Multiple Comparison with significant ($p < 0.05$).

3. Results and Discussion

Figure 6 (a) illustrates soy milk deposited on SS during the heating process. As seen in the figure, the formation of soy milk deposit was clearly observed as a soft deposit at 30 min. After 60 minutes soy milk deposit was more dense film-like. Changes in surface characteristics of sample plates were also noticed from infrared thermography as presented in Figure 6 (b). Generally, an area having the purple or blue color tone indicates the area emitted the infrared radiation lower than an area having red or green or yellow tone. According to ε value of SS was lower than soy milk deposits, the whole area of thermal image at 0 min. (clean SS) displayed in blue color tone. Area of blue color reduced with time, meanwhile area of green and yellow increased. Until 120 - 150 min most area of SS was covered with soy milk deposits as shown in yellow color. At 180 min., thermo-map of SS presented in red color. This means soy milk film was created and covered the total area of SS.

For 180 min. of process, soy milk deposits showed insignificant soiling on both grades of SS plates, but they showed significant soiling with increasing of R_a as shown in Table 1. The results could be summarized that the surface roughness was the affecting factor to the deposits of organic matter rather than the grade of stainless steel. The findings are also reported by Dürr [7].

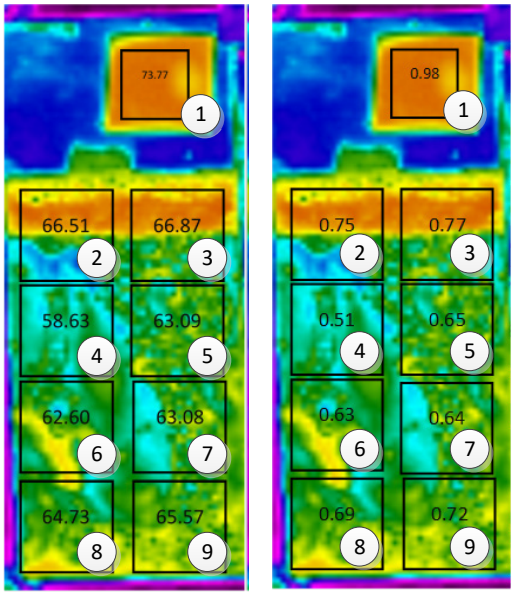

(a) (b)

Figure 5. Averaged surface temperature (a) and ε values (b) at each ROI

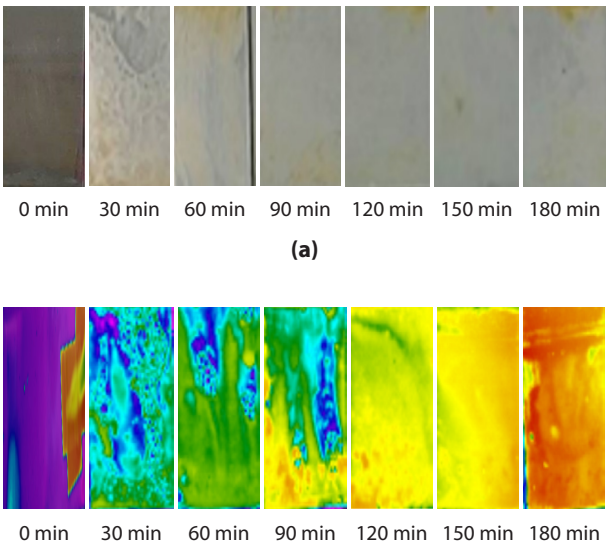

Figure 6. Optical images (a) and thermal images (b) of soy milk deposited on SS AISI 304 - 0.4 µm Ra

Table 1. The accumulation of deposited soy milk for 3 hours

Type of stainless steel	Average roughness (μm)	Mass of deposits (g)
AISI 304	0.4	0.27 ± 0.01[a]
	0.8	0.29 ± 0.00[b]
	3.2	0.39 ± 0.03[c]
AISI 316	0.4	0.26 ± 0.02[a]
	0.8	0.29 ± 0.01[ab]

[a, b, c]: Statistically significant difference ($p \leq 0.05$).

During heating process, mass of soy milk deposits was observed and ε value was simultaneously computed in real-time by computer vision acquiring the infrared thermography from a thermal image camera. The minimum *e* value was found at 0 min. indicating the clean SS. That means only the radiation of SS captured by infrared camera. The ε value of SS equals to: 0.34, 044, and 0.61 at 0.4, 0.8, and 3.2 μm R_a, respectively [16, 20]. The ε value of sample plates increased with time until it reached to ε value of soy milk film, equals to 0.95. This could be interpreted as the soy milk deposits was fully covered over the surface. Change in ε values with time at each R_a was in accord with change in mass of the deposits as shown in Figure 7. Therefore, it could be concluded that increasing of the deposits on the SS results in increasing of ε values in the linear relationship with R^2 more than 0.9 as presented in Figure 8.

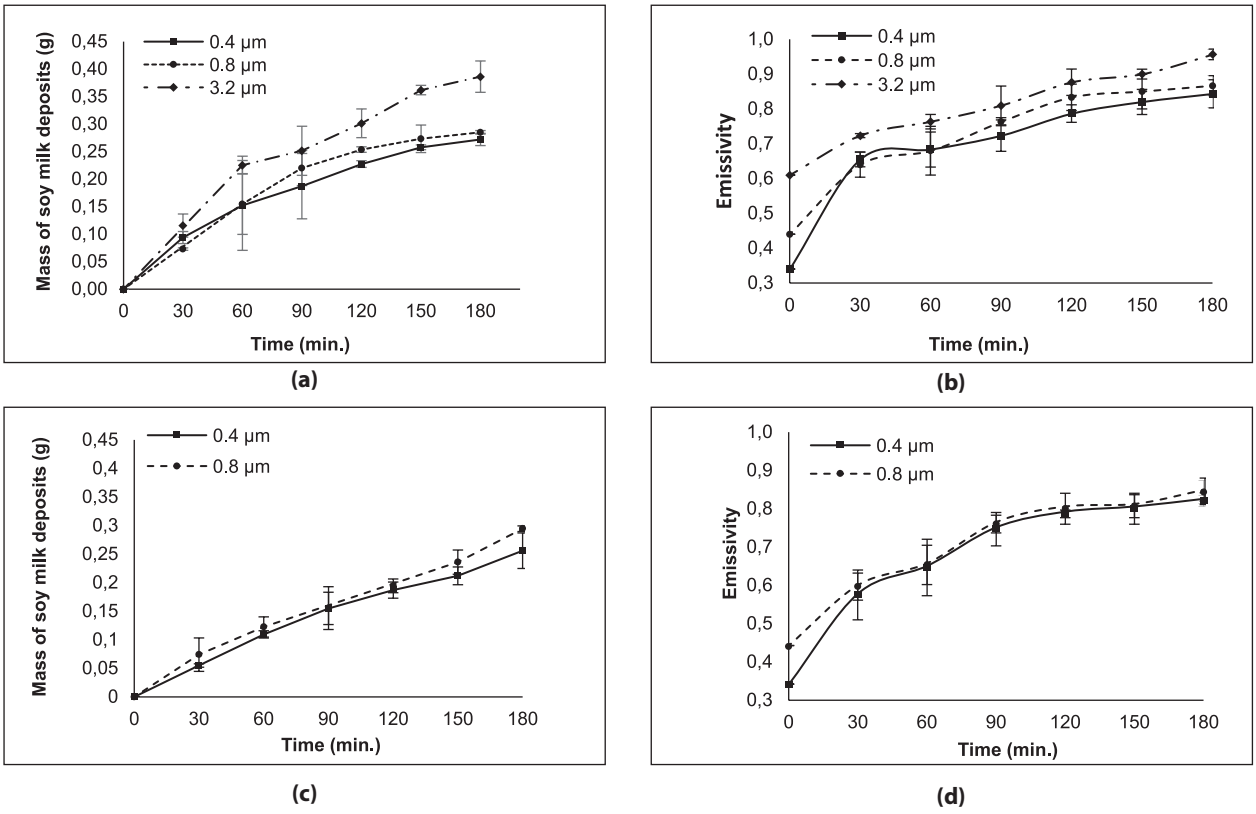

Figure 7. Mass of soy milk deposited on SS and e values of sample plates of AISI 304 (a, b) and AISI 316 (c, d) at various Ra values

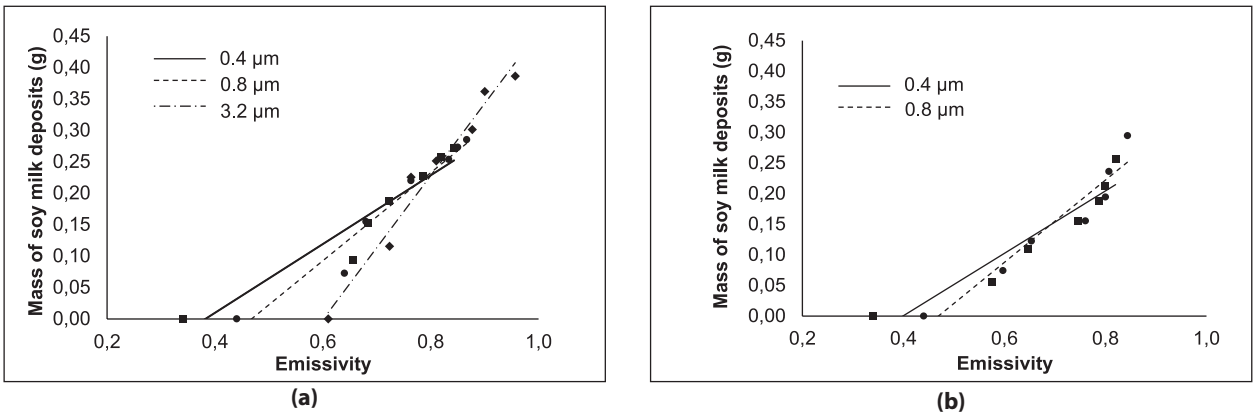

Figure 8. Relationship between e values and soy milk deposits on SS AISI 304 (a) and AISI 316 (b) at various Ra values

4. Conclusions

- This research has developed the real-time investigation method of organic fouling on food contact surface by considering the relationship between ε value and mass of soils on the surface using a thermal image processing technique.

- The soy milk deposited on two grades of SS with various average surface roughness was used as a case for studying the organic fouling behavior. From experiments it was found that soiling on SS could be detected in real-time by the investigating of ε values changes during process time.

- ε of SS having soil on the surface was higher than a clean SS since the soil film on the SS caused the roughness of surface to be changed. According to the result of soil mass determination, it could be concluded that increasing of the deposits on the SS results in increasing of ε values in the linear relationship with R^2 more than 0.9. Therefore, it could be concluded that the proposed technique was possible to investigate the accumulation of soy milk and other soil types on the surface.

- Our scheme is very useful for developing the cleaning system in food industry. However, factors related to measurement accuracy such as the reflection from surrounding and average temperature values obtained by the region of interest need to be considered. When the ROI was created covering low and high infrared energy, the emissivity could be error because the temperature was not homogenous.

5. References

[1] Jullien C., Benezech T., Carpentier B., Lebret V., Faille C. (2002). *Identification of surface characteristics relevant to the hygienic status of stainless steel for the food industry*. Journal of food engineering, 56, pp. 77-87.

[2] The European Parliament and Council of the European Union. (2006). *Directive 2006/42/EC on machinery, and amending Directive 95/16/EC*. OJ. L. 157.

[3] EHEDG. (2004). *Document No. 8: Hygienic Equipment Design Criteria* (2nd Ed.).

[4] Vanhaecke E., Remon J. P., Moors M., Raes S., Rudder D. D., Peteghem A. V. (1989). *Kinetics of Pseudomonas Aeruginosa Adhesion to 304 and 316-L Stainless Steel: Role of Cell Surface Hydrophobicity*. Applied and Environmental Microbiology, 56, pp. 788-795.

[5] Boyd R. D., Verran J., Hall K. E., Underhill C., Hibbert S., West R. (2000). *The cleanability of stainless steel as determined by photoelectron spectroscopy*. Applied Surface Science, 172, pp.135-143.

[6] Foschino F., Picozzi C., Civardi A., Bandini M., Faroldi P. (2003). *Comparison of surface sampling methods and cleanability assessment of stainless steel surfaces subjected or not to shot peening*. Journal of Food Engineering, 60, pp. 375-381.

[7] Dürr H. (2007). *Influence of surface roughness and wettability of stainless steel on soil adhesion cleanability and microbial in-activation*. Food and Bioproducts Processing, 85, pp. 49-56.

[8] Mairal A.P., Greenberg A.R., and Krantz W.B. (2000). Investigation of membrane fouling and cleaning using ultrasonic time domain reflectometry. Desalination 130, pp. 45 – 60.

[9] Meng F., Liao B., Liang S., Yang F., Zhang H., Song L. (2010). *Morphological visualization, componential characterization and microbiological identification of membrane fouling in membrane bioreactors (MBRs)*. Journal of Membrane Science, 361, pp. 1-14.

[10] Ndukaife K. O., Ndukaife J. C., Agwu Nnanna A. G. (2015). *Membrane fouling characterization by infrared thermography*. Infrared Physics and Technology, 68, pp.186-192.

[11] Senni L., Ricci M., Palazzi A., Burrascano P., Pennisi P., Ghirelli F. (2014). *On-line automatic detection of foreign bodies in biscuits by infrared thermography and image processing*. Journal of Food Engineering, 128, pp.146-156.

[12] Nunak T., Rakrueangdet K., Nunak N., Suesut T. (2015). *Thermal Image Resolution on Angular Emissivity Measurements using Infrared Thermography*. Proceedings of The International MultiConference of Engineers and Computer Scientists, Hong Kong, pp. 323-327.

[13] Svantner M., Vacikova P., Honner M. (2013). *Non-contact charge temperature measurement on industrial continuous furnaces and steel charge emissivity analysis*. Infrared Physics Technology 61, pp. 20-26.

[14] Marinetti S., Cesaratto P. G. (2012). *Emissivity estimation for accurate quantitative thermography*. NDT&E International, 51, pp. 127-134.

[15] Nunak T., Nunak N., Tipsuwanporn V., Suesut T. (2015). *Surrounding Effects on Temperature and Emissivity Measurement of Equipment in Electrical Distribution System*. Proceedings of the World Congress on Engineering and Computer Science, San Francisco, USA, pp. 21-23.

[16] Suesut T., Nunak N., Nunak T., Rotrugsa A., Tuppadung Y. (2011). *Emissivity Measurements on Material and Equipment in Electrical Distribution System*. 11th International Conference on Control Automation and Systems Proceedings, Gyeonggi-do, Korea, pp. 1259-1263.

[17] Lopez A., Molina-Aiz F. D., Valera D. L., Pe na A. (2012). *Determining the emissivity of the leaves of nine horticultural crops by means of infrared thermography*. Journal of Scientia Horticulturae, 137, pp. 49-58.

[18] Yu D. U., Shrestha B. L., Baik O. D. (2015). *Thermal conductivity, specific heat, thermal diffusivity, and emissivity of stored canola seeds with their temperature and moisture content*. Journal of Food Engineering, 165, pp. 156-165.

[19] Brosnan T., Sun D. W. (2002). *Inspection and grading of agricultural and food products by computer vision systems - A review*. Computers and Electronics in Agriculture, 36, pp. 193-213.

[20] Shi D., Zou F., Wang S., Zhu Z., Sun J. (2014). *Effect of surface oxidation on the spectral emissivity of steel 304 at the elevated temperature in air*. Infrared Physics, 66, pp. 6-12.